AGU ADVANCING EARTH AND SPACE SCIENCE

Geophysical Research Letters

RESEARCH LETTER
10.1029/2020GL090999

African Low-Level Jets and Their Importance for Water Vapor Transport and Rainfall

Callum Munday[1], **Richard Washington**[1], **and Neil Hart**[1]

[1]School of Geography and the Environment, University of Oxford, Oxford, UK

Key Points:

- Topographically constrained nocturnal low-level jets dominate water vapor transport from the Indian Ocean to the African interior
- Drought is prevalent in the jet entrance regions across eastern and southern Africa during years with strong jets
- Coarse resolution climate models do not simulate key low-level jets: A failure which contributes to errors in simulated rainfall

Supporting Information:

- Supporting Information S1

Correspondence to:
C. Munday,
callum.munday@ouce.ox.ac.uk

Citation:
Munday, C., Washington, R., & Hart, N. (2021). African low-level jets and their importance for water vapor transport and rainfall. *Geophysical Research Letters*, *48*, e2020GL090999. https://doi.org/10.1029/2020GL090999

Received 30 SEP 2020
Accepted 7 DEC 2020

Abstract Uncertainty in the future evolution of tropical rainfall is linked to circulation changes under warming. In Africa, a key barrier to interpreting rainfall changes is our limited understanding of water vapor transport across the continent. Here, we show that a series of nocturnal easterly Low-Level Jets (LLJs), which form in the valleys punctuating the East African rift system, transport the majority of water vapor to central Africa from the Indian Ocean. There is a robust connection between strengthened LLJs and drought in eastern and southern Africa at interannual timescales, mediated by an increase in low-level divergence and water vapor export. Analysis of climate model simulations at a wide range of resolutions (250–4.5 km) suggests that grid lengths <60 km are needed to simulate the salient structures of LLJs. The failure of coarse resolution models to capture LLJs is linked with biases in rainfall climatology and variability across the continent.

Plain Language Summary Africa is one of the continents least responsible for climate change but will bear a disproportionate share of its impact, particularly through changes to droughts and floods. An important task for climate scientists is therefore to understand possible future changes to African rainfall. Unfortunately, this task is made difficult by large gaps in our knowledge of the basic mechanics of the climate system over Africa. One of these gaps is in our understanding of how water vapor—which is a key ingredient for rainfall—travels from the Indian Ocean into the African interior. Here, we show that over 200,000 tonnes of water vapor are transported each second through a series of invisible rivers, which flow through the atmosphere in valleys interrupting the high mountains of the East African Rift System. The models that we use to project rainfall change can capture the structure of these invisible rivers, but only if they represent the mountains of tropical Africa realistically.

1. Introduction

Africa is the continent least responsible for anthropogenic climate change but will bear a disproportionate share of its impact. This is due to both the expected severity of climate change (Collins et al., 2013) and high-economic exposure to climatic variation (Collier et al., 2008). Some of the impact can be alleviated by climate adaptation (e.g., Conway et al., 2015), but the efficacy of adaptation rests on the availability of credible climate information at the regional scales relevant for decision making (James et al., 2017). The pressing need for reliable climate information sits uncomfortably alongside large gaps in our understanding of some of the basic mechanics of the African climate system.

One such gap is in our understanding of water vapor transport over the continent. Giannini et al. (2018) shows that projections of wetting in East Africa among coarse resolution climate models are associated with reductions in easterly water vapor transport across the East African Rift System (EARS) toward Central Africa. Such easterly water vapor transports are a key source of moisture for Central Africa (Dyer et al., 2017; Sorí et al., 2017; Van Der Ent & Savenije, 2013). However, the ability of models to simulate the preferred locations and mechanisms of water vapor transport is unknown, in part because we do not know what they are in reality (Giannini et al., 2018). In the Andes and Himalayas, areas of similar topographic complexity, the water vapor transports are associated with topographically constrained flows—often through Low-Level Jets (LLJs) (Acosta & Huber, 2017; Jones, 2019). Models of coarse resolution often struggle to capture the LLJs (Acosta & Huber, 2017).

While easterly transport from the Indian Ocean is an important source of moisture for Central Africa, enhanced easterly winds emanating from the Indian Ocean are commonly associated with drought across

eastern and southern Africa (Dezfuli & Nicholson, 2013; Finney et al., 2019; Makarau & Jury, 1997; Vizy & Cook, 2019). Moreover, the robust future drying signal in southern Africa in coupled climate models occurs as easterly winds strengthen across eastern parts of the subcontinent (Howard & Washington, 2020; Munday & Washington, 2019). In this study, we consider the role of these easterlies, which supply moisture to Central Africa, in eastern and southern Africa drought. We also consider how well climate models capture the key modes of easterly water vapor transport. We answer the following questions:

1. What are the characteristics of water vapor transport into the tropical African interior from the Indian Ocean?
2. Is variability in easterly water vapor transport in key locations associated with rainfall variability in eastern and southern Africa on interannual timescales?
3. Can climate models simulate the correct structure of easterly water vapor transport, and relationships with rainfall variability in eastern and southern Africa?

In answering these questions, we demonstrate a crucial role played by nocturnal easterly LLJs which form in the topographic lows punctuating the EARS. Two of these LLJs: The Turkana Jet (Kinuthia & Asnani, 1982), forming between the Kenyan and Ethiopian highlands; and the Limpopo Jet (Rife et al., 2010; Zunckel et al., 1996), which forms in the Limpopo river valley, have previously been described. To the best of our knowledge, the other LLJs—which we refer to as the Zambezi Jet, the Rufiji Jet, and the Malawi Jet—remain undocumented in the academic literature.

2. Data and Methods

NASA's high-resolution MERRA2 reanalysis data (1981–2017, 0.5 × 0.625° latitude and longitude) is used to sample the circulation. MERRA2 performs well in comparison to observations over tropical Africa (Hua et al., 2019; Vellinga & Milton, 2018) and is in broad agreement with the latest ECMWF reanalysis data set (ERA5, 0.28125 × 0.28125° latitude and longitude) in its simulation of the LLJs (Figure S1). Rainfall (1981–2017) is estimated using the high-resolution Climate Hazards Group InfraRed Precipitation with Station Data (CHIRPS) data set (Funk et al., 2015). By comparing the CHIRPS data set with 1,200 independent stations in East Africa, Dinku et al. (2018) demonstrate that rainfall biases in CHIRPS are small, and at monthly timescales is lower than in similar high-resolution satellite data sets.

Section 5 evaluates the climate model simulation of the LLJs. We use the historical experiment (1980–2005) for 25 global models from phase 5 of the Coupled Model Intercomparison Project (CMIP5; Table S1) and a 30 years global model simulation of the Met Office Unified Model (UM) Global Atmosphere 7.0 (GA7) at N512 resolution forced by daily sea surface temperatures from a 0.25° spatial grid. We additionally analyze a limited-area model over a Pan-Africa domain, at 4.5 km grid spacing with explicit simulation of convection (CP4-Africa). It is forced at its lateral boundaries by the global model (GA7) for a 10 years climatology. Stratton et al. (2018) reports the full details of the experiment.

Vertically integrated water vapor transport is calculated at three hourly intervals from surface to 700 hPa as follows:

$$\boldsymbol{QV} = \int_{Ps}^{700} q\boldsymbol{V}\frac{dP}{g} \tag{1}$$

where

$$\boldsymbol{QV} = \left(Qu, Qv\right)$$

$\boldsymbol{V} = \left(u, v\right)$, q is the specific humidity, g is the gravitational acceleration, P is pressure, and P_s is surface pressure. The 700 hPa level is chosen as it is the upper limit of the LLJs. In Section 5—for comparison with monthly mean CMIP5 data—we recalculate the MERRA2 integrated transport at monthly intervals.

Cross sections are defined separately for each jet (Table S2). To calculate the water vapor transport for each jet we find the scalar of $\boldsymbol{QV}$ normal to each cross section:

$$\boldsymbol{QV}_l = -Qu\sin\theta + Qv\cos\theta \quad (2)$$

where

$$\theta = \tan^{-1}\left(\frac{ly}{lx}\right)$$

ly and *lx* are the length of the jet latitude and longitude segments (Table S2). We then interpolate $\boldsymbol{QV}_l$ to the cross section, before integrating across the length of cross section to obtain the water vapor mass flux associated with the jet (with units of kg s^{-1}). In Section 4.2, the regional moisture budget is calculated by summing the water vapor mass flux import/export across the boundaries shown Figure S3.

3. African Low-Level Jets and Water Vapor Transport

The annual mean vertically integrated water vapor flux is easterly across tropical Africa (Figure 1a). There are five low-level jets associated with this transport in the valleys along the EARS (Figure 1b), namely: (from north to south) the Turkana Channel, Rufiji Basin, Malawi, The Zambezi river valley, and the Limpopo river valley. Peak annual mean wind speeds of ~11 m s^{-1} occur at night (Figure 1c) within 1.5 km above the surface, with wind speeds decreasing rapidly above. This is classic structure for low-level jets (Bonner, 1968), and the >50% reduction in strength during the day (Figure 1d) is consistent with LLJs globally (e.g., Blackadar, 1957; Rife et al., 2010; Van der Wiel et al., 2015).

The Turkana Jet (2°N, 36°E) is the strongest of the LLJs. Annual mean water vapor transport is 6.5×10^7 kg s^{-1} (Table S2) through the ~600-km-wide channel. Vizy and Cook (2019) and Nicholson (2016) suggest that the Turkana Jet contributes to regional aridity, through enhancing divergence in the jet entrance region. Farther south, two easterly LLJs form over the Rufiji Basin in Central Tanzania (4°S, 35°E) and in Malawi (12°S, 32.5°E). Annual mean water vapor mass flux is 5.0×10^7 kg s^{-1} and 3.7×10^7 kg s^{-1} for the Rufiji and Malawi LLJ, respectively. Like the Turkana Jet, these LLJs are tied to the topography. The Malawi LLJ forms to the south of the Tanzanian Escarpment, while the Rufiji LLJ is bounded to its north by the Kenyan Highlands and its south by the Tanzanian Escarpment. Comparison with the higher resolution ERA5 data (Figure S1) shows that the Rufiji Jet itself consists of at least three distinct jets which form in saddles of the Tanzanian Highlands.

In southeastern Africa, two LLJs are present. The Limpopo Jet (22°S) sits in the Limpopo River valley and is the weakest of the five LLJs. To the north, one further jet forms in the Zambezi River Valley—the Zambezi LLJ. In September 1992, a westward extension of this LLJ is likely to have been sampled with aircraft observations and pilot balloon tracking near Victoria Falls in Zimbabwe (Meixner et al., 1993, cited in; Zunckel et al., 1996). The annual mean water vapor flux across the Zambezi channel is 5.1×10^7 kg s^{-1}, over double that of the Limpopo Jet (2.3×10^7 kg s^{-1}).

The presence of LLJs in the valleys punctuating EARS suggests that the fast wind speeds are, in part, a consequence of channeling of the flow (i.e., Bernoulli Effect). Indeje et al. (2001) show this experimentally for the Turkana Jet, which reduces in speed in a model setup with a shallower valley between the Kenyan and Ethiopian Highlands (Indeje et al., 2001)

4. Variability of LLJs and African Rainfall

This section considers the variability of the LLJ water vapor transport across the annual cycle and its variability from year to year.

4.1. Annual Cycle

The lower-tropospheric integrated (surface to 700 hPa) water vapor flux associated with the LLJs varies by a factor of three through the year (Figure 2). For four of the jets (Turkana, Rufiji, Malawi, and Zambezi) the annual cycle is bimodal with distinct peaks in March to May (MAM) and September to November (SON)

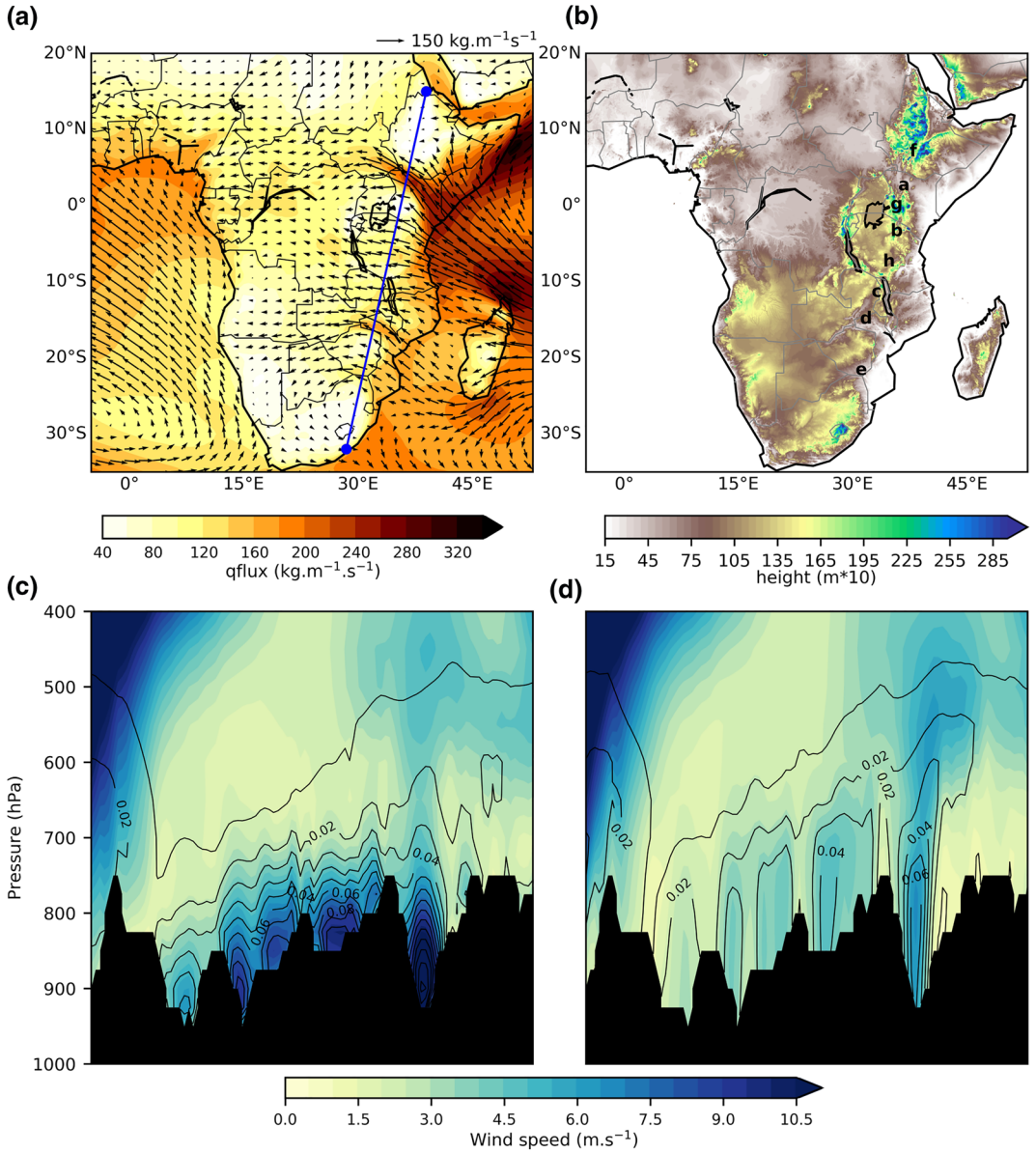

Figure 1. (a) Vertically integrated water vapor transport to 700 hPa (shaded; kg m s^{-1}) with vectors of integrated water vapor transport. (b) African surface height (USGS—GTOPO30), units in m*10. Labels *a*–*e* are for LLJs: (*a*) Turkana; (*b*) Rufiji; (*c*) Malawi; (*d*) Zambezi; (*e*) Limpopo. Labels *f*, *g*, and *h* show orographic features: Ethiopian Highlands; Kenyan Highlands; and Tanzanian escarpment, respectively (c) 00:00 UTC and (d) 12:00 UTC vertical section through atmosphere of windspeed (shaded; m s^{-1}) and water vapor flux (contours; kg m s^{-1}) along blue line in (a) (15°N; 39°E-32°S; 28.5°E). LLJs, Low-Level Jets.

(Figure S2). In SON and MAM, the combined mean water vapor mass flux for these LLJs is between 2 and 3×10^8 kg s^{-1} (Figure 2). During the minima, in July-August and January-February, total LLJ-related water vapor transport decreases by 30%–50%. The water vapor transport associated with the Limpopo jet (at 22°S) displays unimodal cycle, peaking during December-February (Figure S2).

The annual cycle in LLJ-related water vapor transport is in phase with the annual cycle in Congo Basin precipitation ($r = 0.86$; $p < 0.001$, $n = 12$; Figure 2). The Congo Basin dry seasons (DJF; JJA) occur when LLJ-related water vapor transport is relatively weak, whereas the wet seasons (MAM; SON) occur when it is strong. Low-level westerlies (which occur below 900 hPa) across the Atlantic Ocean coast are also considered to be an important water vapor source for Congo Basin rainfall (Cook & Vizy, 2016; Pokam et al., 2014).

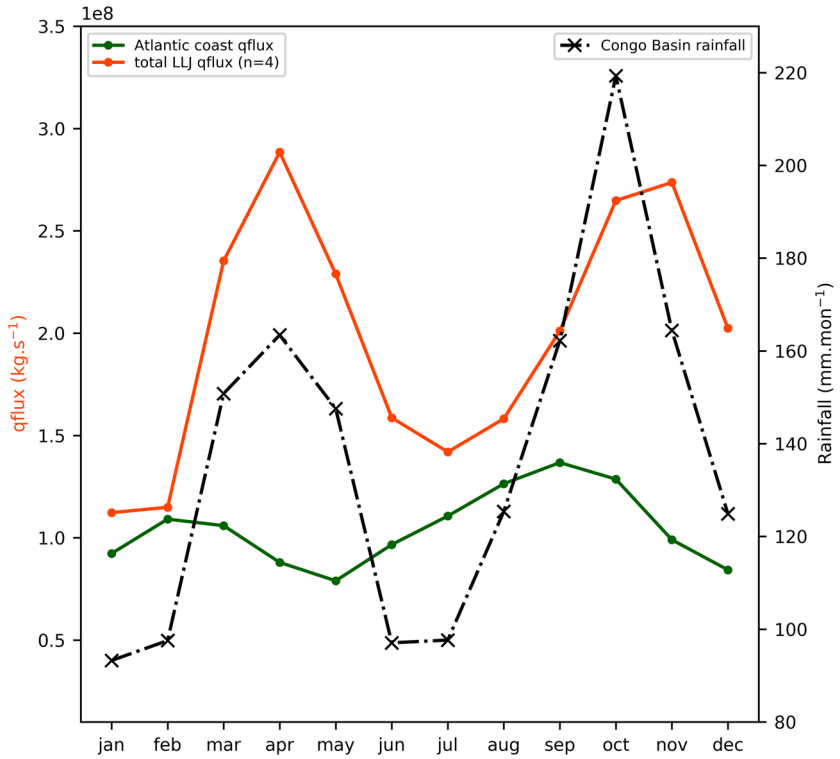

Figure 2. Annual cycle in water vapor flux and Congo Basin rainfall. Orange line is the sum of the water vapor mass flux (kg s^{-1}) integrated from surface to 700 hPa for four LLJs: Turkana, Rufiji, Malawi, and Zambezi. The green line shows total water vapor mass flux (kg s^{-1}) across Atlantic coast (6°N–16°S) associated with low-level westerlies integrated from surface to 900 hPa. The dotted-dashed line is Congo Basin rainfall (12–28°E; 7°S–7°N) in mm month^{-1}. LLJs, Low-Level Jets.

Figure 2 shows that the net low-level westerly water vapor transport is weaker than jet-related transport throughout the year, including by a factor of 2.5–3 during the peak of the Congo Basin rainfall seasons (April and October). The results are consistent with previous studies, which show that the Indian Ocean is the major moisture source for the Congo basin (Dyer et al., 2017; Van Der Ent & Savenije, 2013).

4.2. Interannual Variability

The mean state of water vapor transport into Africa is dominated by LLJs. In this section, we show that the interannual variability of the Turkana, Malawi and Zambezi jets is associated with the contemporaneous modulation of rainfall. We consider anomalies in rainfall, circulation and moisture budget during a composite of eight years when the LLJs are strongest compared to the eight years when they are weakest, as measured by wind speed at the core of each LLJ (Table S2). For clarity, we focus on a single month in the local rainy season when the jet is present and where the monthly coefficient of variation (1981–2017) is greater than 30%: April for the Turkana Jet, December for the Malawi Jet and February for the Zambezi Jet.

In all three cases, a stronger LLJ is associated with rainfall deficits of 60–130 mm month^{-1}, both upstream and in the region of the jet (Figure 3). The drier conditions are associated with faster easterly winds resulting in anomalous low-level (850 hPa) divergence in the jet entrance and core regions (Figure S3). In the case of the Malawi and Zambezi LLJs, the acceleration of winds is supported by high pressure ridging over the eastern African coast (Figure S3). The results for Turkana are consistent with analysis of other months in Nicholson (2016) and Vizy and Cook (2019).

To clarify the contribution of the jets to drought in eastern Africa, we calculate the moisture budget of the regions defined by the negative rainfall anomalies (Figure 3)—with longitudes ranging from eastern coastline to jet core (regions shown in Figure S3). Table S3 quantifies the moisture budget, and the contribution

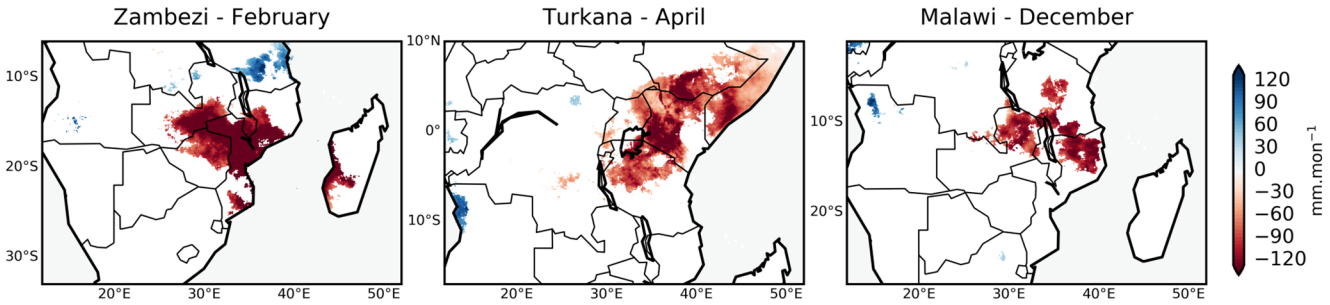

Figure 3. Composite anomaly for rainfall in 8 months with strongest LLJ minus 8 months with weakest LLJ (1981–2017). Areas which are not significant based on Students *t*-test are masked, with significance assessed after controlling for the false discovery rate (FDR) following Wilks (2016), with a control FDR value of αFDR = 0.1. LLJs, Low-Level Jets.

of LLJs to moisture export. For the monthly climatology (1981–2017), the Turkana (April), Malawi (December), and Zambezi (February) jets contribute 63%, 65%, and 51% to the export of water vapor in the regions of negative rainfall anomalies, respectively. The LLJs are therefore key contributors to the average moisture export. During years with strong compared to weak jets, there is anomalous export of water vapor from the jet entrance regions contributing to the negative rainfall anomalies. The faster LLJ-related water vapor export accounts for 62%, 95%, and 53% of the anomalous moisture export for the regions upstream of the Turkana, Malawi and Zambezi Jet, respectively.

We do not find that the enhancement in easterly transport across the rift system results in a clear, spatially extensive increase Congo Basin rainfall. The variability in westerly transport from the Atlantic (Cook & Vizy, 2016; Pokam et al., 2014) could play a more significant role, although as Dyer et al. (2017) argues this the role of westerlies could be in increasing low-level convergence rather than in the provision of water vapor.

5. Model Simulation of LLJs and Rainfall Biases

The role of water vapor transport by LLJs on mean and interannual time scales is clear. Are climate models able to capture the LLJs and is there a relationship with model resolution? Both the high-resolution global model N512 (~25 km) (GA7), and the convective permitting 4.5 km resolution model (CP4-Africa) simulate distinct LLJs (Figures 4a and 4b). Compared to MERRA2 at 50 km grid length, the higher resolution of GA7 and CP4 enables four further topographically bound LLJs to be resolved. These form in the saddles of the Tanzanian highland topography between 2°S and 10°S and are embedded jets within the wider Rufiji LLJ.

The topographic constraint on the LLJs is too weak in coarser resolution CMIP5 models. In a composite of Lowest Resolution (LR; >200 km grid) CMIP5 models, the distribution of LLJs is poorly represented (Figures 4c and 4d). In the LR model-set the Turkana Jet is distinguishable as a discrete maximum, but the four separate jets south of the equator present as a broad horizontal maximum. Higher resolution (HR) CMIP5 models—with grid spacing 100 km or less—improve modestly on this performance, simulating a distinct Turkana Jet and two other jets further south.

To clarify how resolution affects LLJ simulation, we assess the relationship between model/reanalysis grid length and the number of LLJs forming across EARS (Figure 4e), with distinct LLJs identified by a closed contour of at least 4 m s^{-1} below 650 hPa. As average grid length decreases, the number of distinct LLJs increases ($r_s = -0.86$, $p < 0.0001$, $n = 29$). The coarsest resolution CMIP5 models simulate two distinct jets across EARS; ERA5 (22 km) simulates eight; and GA7 (25 km) and CP4 (4.5 km) both simulate nine.

The failure of CMIP5 models to accurately simulate the distinct LLJs results in circulation biases that are consequential for model rainfall (Figure 5). For the annual mean, the CMIP5 ensemble mean model features weak convergence of vertically integrated moisture across the majority of eastern and southern Africa. MERRA2 simulates a more complicated pattern: regions of moisture divergence associated with each of the five LLJs are interrupted by relatively smaller areas of intense moisture convergence. The missing jet-related divergence in the ensemble mean model contributes to an overestimation of annual mean rainfall across

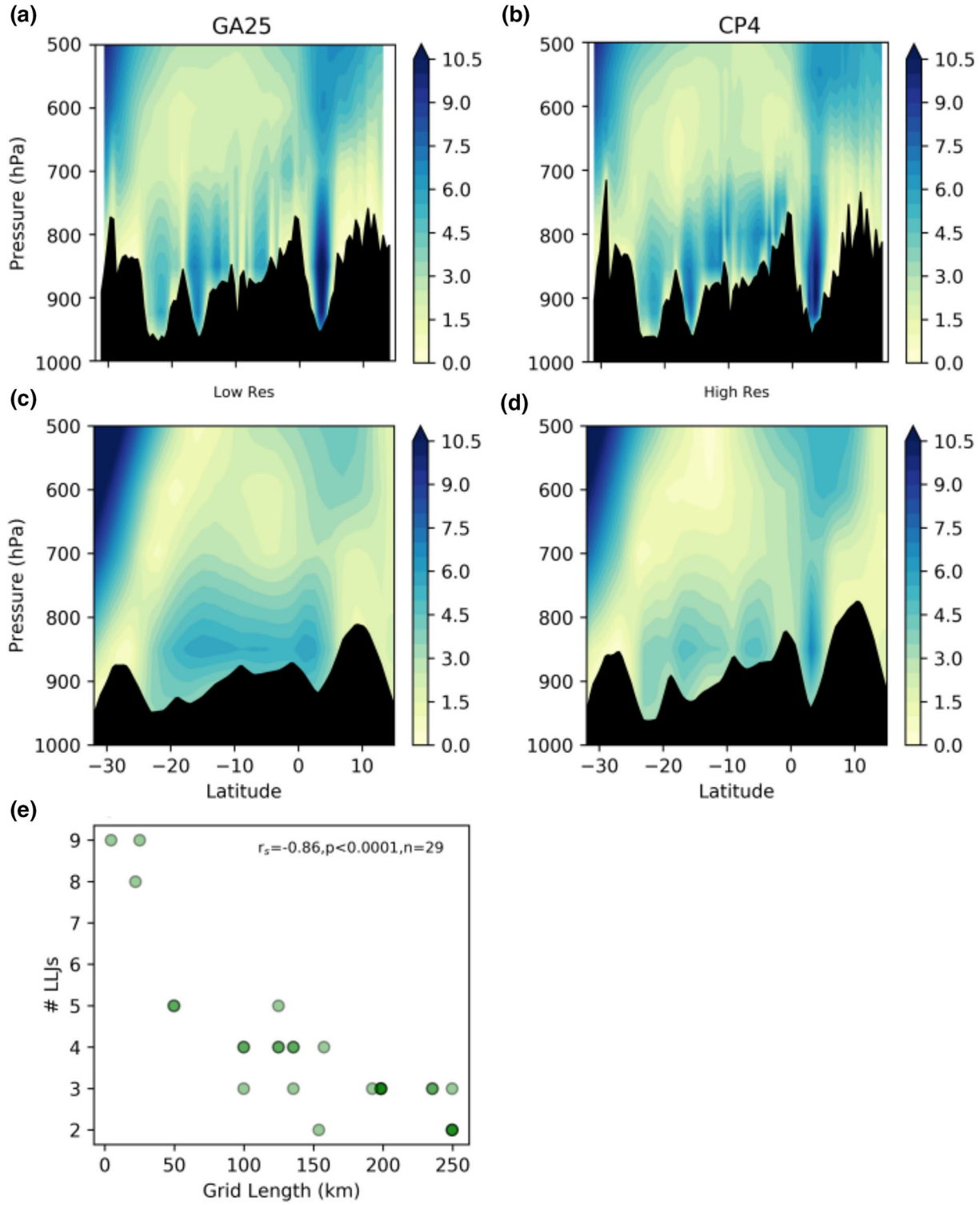

Figure 4. Cross section along blue line in Figure 1a of wind speed (m s^{-1}; shaded) in (a) GA25, (b) CP4, (c) low-resolution, and (d) high-resolution CMIP5 models (1980–2005). (e) The relationship between model and reanalysis average grid length (total number of grids divided by Earth surface area) and number of LLJs across EARS. The Spearman's rank correlation coefficient (r_s) is displayed. Dots of darker colors indicate where more than one model/reanalysis has the same grid length/number of LLJs. CMIP5, Coupled Model Intercomparison Project; EARS, East African Rift System; LLJs, Low-Level Jets.

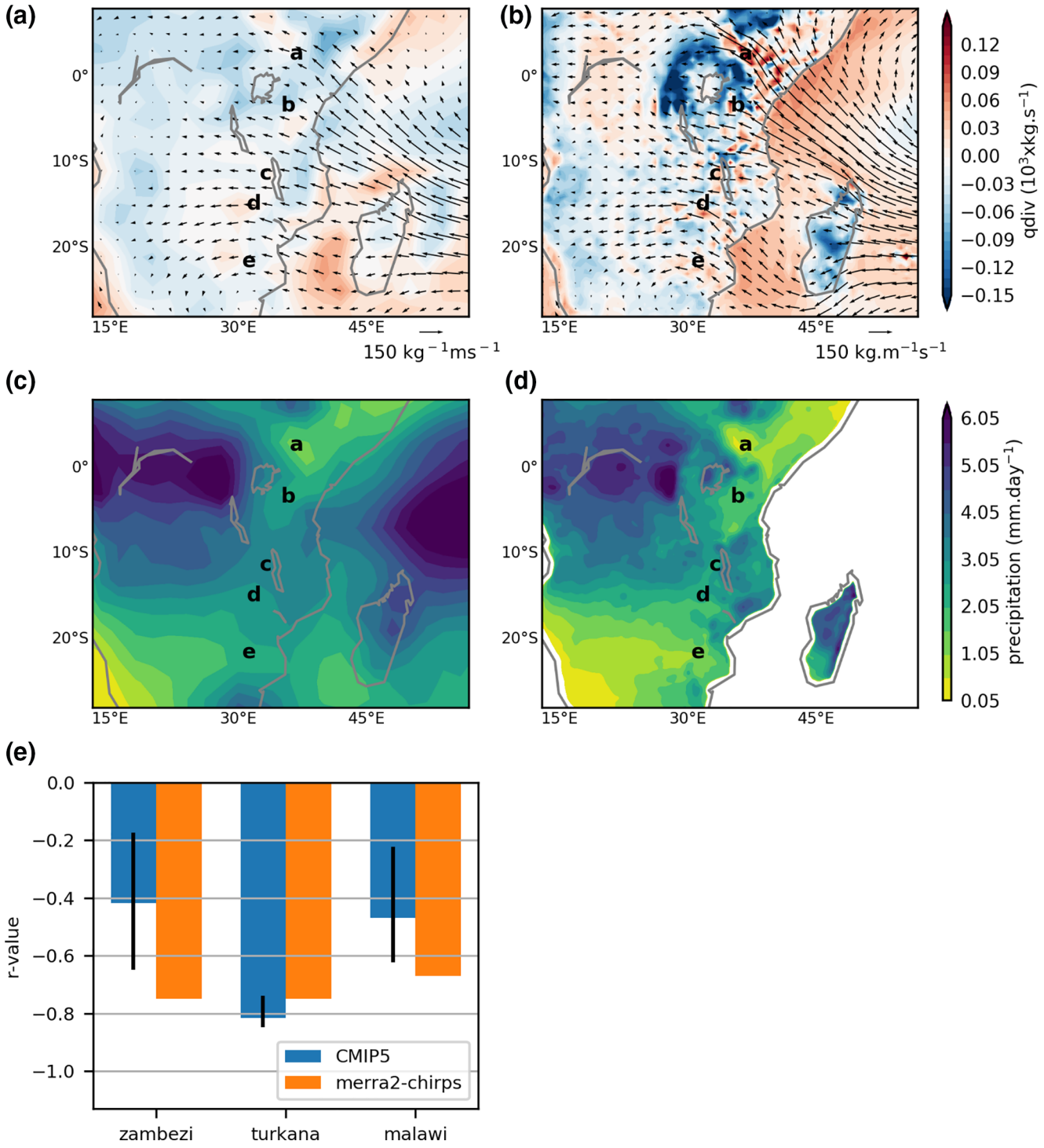

Figure 5. Annual mean divergence of vertically integrated water vapor flux (kg s^{-1}; shaded) and vectors of the integrated water vapor transport in (a) CMIP5 ensemble mean (1980–2005) and (b) MERRA2. Second row shows annual mean rainfall climatology in (c) CMIP5 ensemble mean and (d) CHIRPS. Panel (e) shows the Pearson's correlation coefficient (r) between strength of the LLJs and rainfall in regions upstream of jet (defined in Table S2) for median CMIP model (blue) and for MERRA2-CHIRPS (1981–2005) (orange). Black bars show model interquartile range. CMIP5, Coupled Model Intercomparison Project; CHIRPS, Climate Hazards Group InfraRed Precipitation with Station Data; LLJs, Low-Level Jets.

the majority of eastern and southern Africa (Figures 5c and 5d), which is particularly prominent in the jet regions. For example, rainfall in the Turkana Channel and Rufiji Basin in the CMIP5 ensemble mean is double CHIRPS data, meanwhile the dry corridor associated with the Zambezi Valley in CHIRPS is missing in the ensemble mean.

Finally, we consider whether CMIP5 models reproduce the correlation between LLJ strength and rainfall in the regions and months defined in Section 4. The models reproduce the magnitude of the negative correlation between the Turkana Jet and April rainfall similarly to MERRA2/CHIRPS (Figure 5e). However, the majority of models underestimate the correlation between easterlies and rainfall for the Zambezi Jet in February and the Malawi Jet in December with 46% and 38% of models, respectively, not showing statistically clear relationships ($p > 0.05, n = 24$). The difficulties in representing this relationship are likely related to the inability of models to simulate these jets, which occupy relatively narrow channels (100–300 km) as compared to the Turkana Channel (600 km). The failure of models to capture this key LLJ-linked rainfall control casts doubt on their ability to quantify future changes in regional variability.

6. Summary and Conclusion

Water vapor transport into the interior of Africa occurs via a series of nocturnal, topographically constrained, easterly LLJs. In combination, the annual mean LLJ transport is 22.6×10^7 kg s^{-1} away from eastern Africa. The annual cycle in LLJ-related water vapor transport is in phase with the annual cycle of Congo Basin rainfall, highlighting the importance of easterly moisture sources for tropical African convection. Alterations to the LLJs on interannual timescales are associated with large-scale rainfall anomalies: years with stronger LLJs tend to be dry in southern and eastern Africa regions (from Kenya to Mozambique) due to the enhanced export of water vapor and increased low-level divergence in the jet entrance and core regions.

The results contribute to an explanation of why eastern tropical Africa relatively dry. In the wet seasons (MAM, SON), when the Somali Jet is not active, the LLJs are responsible for low-level water vapor export from eastern Africa and the acceleration of the flow through valleys is divergent at low-levels in the atmosphere. Divergence in lower-tropospheric levels and deficits of moist static energy are cited as key reasons why East Africa is on the convective margin, even during the rainy seasons (Giannini et al., 2018; Trewartha, 1961; Yang et al., 2015). The ensemble mean CMIP5 model fails to simulate the salient structures of LLJs and moisture divergence, and overestimates rainfall across much of eastern and southern Africa. A more complete understanding of the LLJs, and their variability, should improve our understanding of the curious aridity of Eastern Africa.

In CMIP models, future projections of rainfall in both eastern and southern Africa are linked with changes in the easterly water vapor flux (Giannini et al., 2018; Munday & Washington, 2019). The poor simulation of the LLJs, and the relationship between LLJ variability and rainfall variability, suggests that more needs to be done to build confidence in the GCM-derived projections of rainfall change. Corroboration of the association between future water vapor fluxes changes and rainfall projections in higher resolution simulations—perhaps with the newly available CMIP6 HighResMIP ensemble—could help in this regard. As would investigation of future changes in high-resolution limited-area models, such as the CP4 model used here.

Finally, we show that a large portion of the water vapor transport in Africa occurs across relatively narrow horizontal distances. Direct observations of the LLJs are virtually absent, but are critical for constraining model and reanalysis estimates of the circulation. Planned observational campaigns to sample the LLJs are invaluable in providing fresh insights into the dynamics of African climate.

Data Availability Statement

MERRA2 data are from http://gmao.gsfc.nasa.gov/products/ and ERA5 data are downloaded from https://cds.climate.copernicus.eu/cdsapp#!/home. USGS GTOPO30 global digital elevation model data are from http://earthexplorer.usgs.gov/. CMIP5 data are from the Earth System Grid Federation

(ESGF) (https://pcmdi.llnl.gov/). CP4 and GA25 data are at https://catalogue.ceda.ac.uk/uuid/a6114f2319b34a58964dfa5305652fc6?jump=related-anchor.

Acknowledgments
This document is an output from the NERC/DFID funded UMFULA project (NE/M020207/1) and the REACH programme funded by UK Aid from the UK Foreign, Commonwealth and Development Office (FCDO) for the benefit of developing countries (Programme Code 201880). However, the views expressed and information contained in it are not necessarily those of or endorsed by FCDO, which can accept no responsibility for such views or information or for any reliance placed on them. The authors would like to thank the two reviewers for helpful comments that improved the manuscript.

References

Acosta, R. P., & Huber, M. (2017). The neglected Indo-Gangetic Plains low-level jet and its importance for moisture transport and precipitation during the peak summer monsoon. *Geophysical Research Letters*, *44*, 8601–8610. https://doi.org/10.1002/2017GL074440

Blackadar, A. K. (1957). Boundary Layer wind maxima and their significance for the growth of nocturnal inversions. *Bulletin of the American Meteorological Society*, *38*, 283–290.

Bonner, W. (1968). Climatology of the low level jet. *Monthly Weather Review*, *96*, 833–850. https://doi.org/10.1175/1520-0493(1968)096<0833:COTLLJ>2.0.CO.2

Collier, P., Conway, G., & Venables, T. (2008). Climate change and Africa. *Oxford Review of Economic Policy*, *24*, 337–353. https://doi.org/10.1093/oxrep/grn019

Collins, M., Knutti, R., Arblaser, J., Dufresne, J.-L., Fichefet, T., Friedlingstein, P., et al. (2013). *Long-term climate change: Projections, commitments and irreversibility*. Cambridge, UK and New York, NY, USA: Cambridge University Press

Conway, D., Archer, E., Deryng, D., Dorling, S., Krueger, T., Landman, W. A., et al. (2015). Climate and southern Africa's water-energy-food nexus. *Nature Climate Change*, *5*, 837–846. https://doi.org/10.1038/Nclimate2735

Cook, K. H., & Vizy, E. K. (2016). The Congo basin Walker circulation: Dynamics and connections to precipitation. *Climate Dynamics*, *47*, 697–717. https://doi.org/10.1007/s00382-015-2864-y

Dezfuli, A. K., & Nicholson, S. E. (2013). The relationship of rainfall variability in western equatorial africa to the tropical oceans and atmospheric circulation. Part II: The boreal autumn. *Journal of Climate*, *26*, 66–84. https://doi.org/10.1175/JCLI-D-11-00686.1

Dinku, T., Funk, C., Peterson, P., Maidment, R., Tadesse, T., Gadain, H., &(2018). Validation of the CHIRPS satellite rainfall estimates over eastern Africa. *Quarterly Journal of the Royal Meteorological Society*, *144*, 292–312. https://doi.org/10.1002/qj.3244

Dyer, E. L. E., Jones, D. B. A., Nusbaumer, J., Li, H., Collins, O., Vettoretti, G., &(2017). Congo Basin precipitation: Assessing seasonality, regional interactions, and sources of moisture. *Journal of Geophysical Research: Atmospheres*, *122*, 6882–6898. https://doi.org/10.1002/2016JD026240

Finney, D. L., Marsham, J. H., Walker, D. P., Birch, C. E., Woodhams, B. J., Jackson, L. S., &(2019). The effect of westerlies on East African rainfall and the associated role of tropical cyclones and the Madden-Julian Oscillation. *Quarterly Journal of the Royal Meteorological Society, 146*, 647–664. https://doi.org/10.1002/qj.3698

Funk, C., Peterson, P., Landsfeld, M., Pedreros, D., Verdin, J., Shukla, S., et al. (2015). The climate hazards infrared precipitation with stations—A new environmental record for monitoring extremes. *Scientific Data*, *2*, 1–21. https://doi.org/10.1038/sdata.2015.66

Giannini, A., Lyon, B., Seager, R., & Vigaud, N. (2018). Dynamic and thermodynamic elements of modeled climate change at the east African margin of convection. *Geophysical Research Letters*, *45*, 992–1000. https://doi.org/10.1002/2017GL075486

Howard, E., & Washington, R. (2020). Tracing future spring and summer drying in southern africa to tropical lows and the Congo air boundary. *Journal of Climate*, *33*, 6205–6228. https://doi.org/10.1175/jcli-d-19-0755.1

Hua, W., Zhou, L., Nicholson, S. E., Chen, H., & Qin, M. (2019). Assessing reanalysis data for understanding rainfall climatology and variability over Central Equatorial Africa. *Climate Dynamics*, *53*, 651–669. https://doi.org/10.1007/s00382-018-04604-0

Indeje, M., Semazzi, F. H. M., Xie, L., & Ogallo, L. J. (2001). Mechanistic model simulations of the East African climate using NCAR regional climate model: Influence of large-scale orography on the Turkana low-level jet. *Journal of Climate*, *14*, 2710–2724. https://doi.org/10.1175/1520-0442(2001)014<2710:MMSOTE>2.0.CO;2

James, R., Washington, R., Abiodun, B., Hart, N., Kay, G., Mutemi, J., et al. (2017). Evaluating climate models with an African lens. *Bulletin of the American Meteorological Society*, *99*, 313–336. https://doi.org/10.1175/BAMS-D-16-0090.1

Jones, C. (2019). Recent changes in the South America low-level jet. *Npj Climate and Atmospheric Science*, *2*, 1–8. https://doi.org/10.1038/s41612-019-0077-5

Kinuthia, J. H., & Asnani, G. C. (1982). A newly found jet in north Kenya (Turkana Channel). *Monthly Weather Review*, *110*, 1722–1728. https://doi.org/10.1175/1520-0493(1982)110<1722:ANFJIN>2.0.CO.2

Makarau, A., & Jury, M. R. (1997). Seasonal cycle of convective spells over southern Africa during austral summer. *International Journal of Climatology*, *17*, 1317–1332. https://doi.org/10.1002/(SICI)1097-0088(199710)17:12<1317::AID-JOC197<3.0.CO;2-A

Meixner, F., Ajavan, A. ., Fickinger, T., Joubert, A., & Chadyienya, R. (1993). *Victoria Falls ground monitoring, aircraft ascents and surface exchange measurements of meteorological quantities CO_2 and O_3*. Paper presented at Southern African Fire-Atmosphere Research Initiative (SAFARI) Data Workshop, Stellenbosch, South Africa.

Munday, C., & Washington, R. (2019). Controls on the diversity in climate model projections of early summer drying over southern Africa. *Journal of Climate*, *32*, 3707–3725. https://doi.org/10.1175/JCLI-D-18-0463.1

Nicholson, S. (2016). The Turkana low-level jet: Mean climatology and association with regional aridity. *International Journal of Climatology*, *36*, 2598–2614. https://doi.org/10.1002/joc.4515

Pokam, W., Bain, C. L., Chadwick, R. S., Graham, R., Sonwa, D. J., & Kamga, F. M. (2014). Identification of processes driving low-level westerlies in West Equatorial Africa. *Journal of Climate*, *27*, 4245–4262. https://doi.org/10.1175/JCLI-D-13-00490.1

Rife, D. L., Pinto, J. O., Monaghan, A. J., Davis, C. A., & Hannan, J. R. (2010). Global distribution and characteristics of diurnally varying low-level jets. *Journal of Climate*, *23*, 5041–5064. https://doi.org/10.1175/2010JCLI3514.1

Sorí, R., Nieto, R., Vicente-Serrano, S. M., Drumond, A., & Gimeno, L. (2017). A Lagrangian perspective of the hydrological cycle in the Congo River basin. *Earth System Dynamics*, *8*, 653–675. https://doi.org/10.5194/esd-8-653-2017

Stratton, R. A., Senior, C. A., Vosper, S. B., Folwell, S. S., Boutle, L. A., Earnshaw, P. D., et al. (2018). A pan-African convection-permitting regional climate simulation with the met office unified model: CP4-Africa. *Journal of Climate*, *31*, 3485–3508. https://doi.org/10.1175/JCLI-D-17-0503.1

Trewartha (1961). *The Earth's Problem climates*. Madison, WI: The University of Wisconsin Press

Van Der Ent, R. J., & Savenije, H. H. G. (2013). Oceanic sources of continental precipitation and the correlation with sea surface temperature. *Water Resources Research*, *49*, 3993–4004. https://doi.org/10.1002/wrcr.20296

Van der Wiel, K., Matthews, A. J., Stevens, D. P., & Joshi, M. M. (2015). A dynamical framework for the origin of the diagonal south Pacific and south Atlantic convergence Zones. *Quarterly Journal of the Royal Meteorological Society*, *141*, 1997–2010. https://doi.org/10.1002/qj.2508

Vellinga, M., & Milton, S. F. (2018). Drivers of interannual variability of the east African "Long Rains. *Quarterly Journal of the Royal Meteorological Society*, *144*, 861–876. https://doi.org/10.1002/qj.3263

Vizy, E. K., & Cook, K. H. (2019). Observed relationship between the Turkana low-level jet and boreal summer convection. *Climate Dynamics*, *53*, 4037–4058. https://doi.org/10.1007/s00382-019-04769-2

Yang, W., Seager, R., Cane, M. A., & Lyon, B. (2015). The annual cycle of East African precipitation. *Journal of Climate*, *28*, 2385–2404. https://doi.org/10.1175/JCLI-D-14-00484.1

Zunckel, M., Held, G., Preston-Whyte, R. A., & Joubert, A. (1996). Low-level wind maxima and the transport of pyrogenic products over southern Africa. *Journal of Geophysical Research*, *101*, 23745–23755. https://doi.org/10.1029/95jd02602